A New Focus on Groundwater–Seawater Interactions
(Proceedings of Symposium HS1001 at IUGG2007, Perugia, July 2007). IAHS Publ. 312, 2007.

Driving while under the influence: pumping-driven circulation under the influence of regional groundwater flow

M. BAYANI CARDENAS[1] **& JOHN L. WILSON**[2]

1 *Geological Sciences, University of Texas at Austin, Austin, Texas 78712, USA*
cardenas@mail.utexas.edu

2 *Earth and Environmental Sciences, New Mexico Inst. of Mining and Technology, Socorro, New Mexico 87801, USA*

Abstract Regional submarine or ambient groundwater discharge (AGD) along sea coasts interacts with current-driven interfacial pumping of seawater through shallow sediments. We use numerical simulations to investigate this interaction for a turbulent current flowing over dune topography. AGD reduces the extent of the current-topography driven interfacial exchange zone (IEZ) and may prevent its development when AGD overpowers interfacial exchange. Under upwelling-AGD conditions (upward flux of deep groundwater into the water-column), the IEZ is centred on the stoss face of bedforms and AGD occurs near the crest. Under downwelling-AGD conditions (downward flux of seawater deep into the aquifer), the IEZ forms around the crest and water infiltrating along the stoss face into the sediments does not return to the sediment–water interface. The IEZ depth, flux and residence time are functionally related to current Reynolds number (Re). For example, the IEZ water residence time, which follows a power-law distribution, is larger at lower current Re.

Key words interfacial exchange; bedform; groundwater discharge; turbulent flow

INTRODUCTION

Ocean and estuarine water are connected to and interact with coastal groundwater. Regional (0.1–10 km) interactions and connections occur when groundwater discharges as diffuse flow from coastal aquifers (diffuse submarine groundwater discharge) or, when the flow is reversed, through intrusion of seawater into aquifers. Depending on direction, this net deep groundwater flow can be referred to as "groundwater upwelling" into the ocean or estuary, when the flow is upward, or as "groundwater downwelling" when the flow is from the ocean or estuary to the groundwater. Hydrogeologists, who normally work with terrestrial freshwater lakes and streams, refer to these situations as "gaining" or "losing", respectively, where the lake or stream gains water by upward groundwater flow, and loses water to the aquifer by downward flow. This paper will use that terminology, but generalize by referring to both situations as examples of regional ambient groundwater discharge (AGD).

Seawater and groundwater interact locally (0.1–10 m) within permeable bottom sediments through pumping and circulation of seawater from the ocean or estuarine water column, downward through sediments, and back up again into the water column. This small-scale circulation is driven by a combination of waves, tides, and currents (Burnett *et al.,* 2003). This paper focuses on current-driven exchange, caused by the

interaction of the water-column current with bottom topography, and which induces eddies and bottom-pressure variations along the sediment–water interface (SWI). Local-scale downwelling occurs in zones of high bottom-pressure where seawater enters the sediments, while local-scale upwelling of water from the sediments occurs in low-pressure zones. When the sediments are permeable enough, the current-driven bottom-pressure variations drive significant advective transport of seawater across the SWI and through the sediments.

The rates and spatial distribution of local current-topography-driven exchange and regional-scale AGD influence many important biogeochemical and ecological processes taking place along the SWI (Boudreau *et al*., 2001), with measurable impacts from local to global scales for both estuaries (Webster *et al*., 1996) and oceans (Riedl *et al*., 1972). The influence is strongest when advection dominates diffusion. When this happens, insight into understanding and observing the biogeochemistry and ecology requires an appreciation of the hydrodynamics (Burnett *et al*., 2003; Huettel *at al*., 2003). This paper investigates the hydrodynamics of current-bedform driven exchange under the influence of regional ambient groundwater discharge (AGD) when the current is turbulent. When the current is laminar, refer to Cardenas & Wilson (2006, 2007b).

METHODOLOGY

We numerically model the flow above and below SWIs in a two-dimensional cross-section and at steady state (Fig. 1). The procedure and system formulation follows that of Cardenas & Wilson (2007a) where the turbulent water column is governed by the Reynolds-averaged Navier-Stokes (RANS) equations coupled with the k–ω closure scheme (Wilcox, 1991), and the interstitial flow within the sediments is assumed to be Darcian and described by the groundwater flow equation. Briefly, we solve the RANS equations first (using the commercial CFD-ACE+ code) while considering the bottom of the water column (the SWI) to be a no-slip wall. We then impose the RANS-based bottom-pressure solution along the wall as a Dirichlet boundary to the top of the groundwater flow model that represents the sediments (solved via the commercial Comsol Multiphysics code). The lateral boundaries for both domains (water column and sediments) are spatially periodic but with a prescribed pressure drop resulting in mean flow from left to right. This mean flow in the sediments is typically referred to as "underflow". Details (e.g. water depth, water column mean velocity field, etc.) and validation of the methodology are presented in Cardenas & Wilson (2007a), in which we considered current-bedform driven exchange but ignored AGD, and are not repeated here. The main difference between our previous work and this study is that we impose a prescribed flux at the lower boundary of the sediments to represent AGD (compare our Fig. 1 to Fig. 1(c) in Cardenas & Wilson (2007a)). At this boundary, we consider a prescribed flux both into and out of the domain representing, respectively, "gaining" and "losing" water columns. Fluid properties are those of freshwater at 20°C and isothermal conditions are assumed (we ignore effects of salinity and temperature on fluid density and viscosity). The sediment, assumed to be sand, is assigned a homogeneous, isotropic permeability (k) of 10^{-10} m^2 in all simulations. We consider the presence of a triangular bedform along the SWI with length L of 1.0 m and height H of 0.05 m, whose crest is invariantly located at 0.9L, typical of subaqueous sand dunes under a unidirectional current.

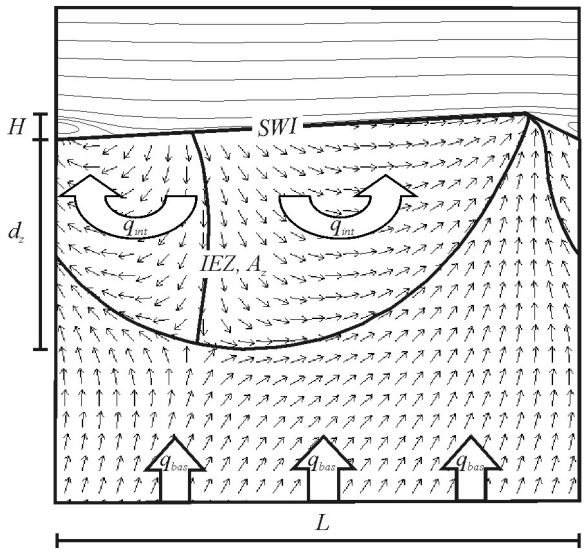

Fig. 1 Schematic representation of the periodic flow domain for the water column and sediments, depicting geometric parameters: height (H) and length (L), and fluxes: basal (q_{bas}) and interfacial (q_{int}). The depth of the interfacial exchange zone (IEZ), d_z, is the vertical distance from the trough to the deepest portion of the streamline enveloping the region wherein water flows from and then back into the water column. Streamlines are presented in the water column while small arrows in the sediments correspond to flow directions but not magnitude. SWI: sediment–water interface.

Sensitivity analysis is performed via multiple CFD simulations by varying the parameter values. We vary the water-column current, measured by a Reynolds numbers (Re), and the prescribed ambient groundwater flux density at the base of the groundwater flow domain, q_{bas}, which we refer to as "basal flux" to differentiate it from other flux terms (Fig. 1). The total basal flux is then given by the product $q_{bas}L$. The Reynolds number is defined as $Re = U_{ave}H/\nu$, where U_{ave} is the average horizontal water-column velocity along a vertical-section taken above the crest of the bedform, and bedform height H is the characteristic length scale. The current U_{ave} and Reynolds number are varied by imposing different horizontal pressure drops across the domain.

RESULTS AND DISCUSSION

We limit our discussion to the flow through the permeable sediments. The water-column current and resulting bottom-pressure distribution are described in Cardenas & Wilson (2007a). The area within the permeable sediments that is physically influenced by current-bedform induced exchange across the SWI is the interfacial exchange zone (IEZ). This is the zone created by the local downwelling of seawater, which then circulates though the sediments and upwells back to the water-column. It is characterized by streamlines that originate and end at the SWI (Fig. 1) and represents the volume of sediments advectively swept by exchanged seawater. Freshwater ecologists and hydrologists commonly refer to this as the "hyporheic zone". The depth of the IEZ, d_z, is taken as the distance between the deepest portion of the streamline which envelopes all streamlines originating from and returning to the SWI, and the

trough of the bedform (Fig. 1). The IEZ flux through the SWI is computed as follows: (i) first, a volumetric flux through the SWI is computed by integration of the magnitude (absolute value) of the normal flux along the bedform surface; (ii) from this we subtract the basal flux ($q_{bas}L$); and (iii) the resulting quantity is divided by two because the integration does not discriminate between current-bedform-driven flux going in and out of the bed, which are in balance. Dividing the IEZ flux by L yields an IEZ flux density, q_{int}, based on bedform length. The total IEZ flux is given by the product $q_{int}L$ and takes place only for that portion of the SWI subjected to current-driven flushing (bounded by the dividing streamline discussed above and illustrated in Fig. 1). The basal and interfacial flux densities, q, which are schematically represented in Fig. 1, are nondimensionalized by $q^* = q/K$, where $K = (kg/\nu)$ is the hydraulic conductivity of the sediments, ν is kinematic viscosity, and g is the acceleration due to gravity.

Flow fields for scenarios with different Re and fixed basal flux, q_{bas}^*, are presented in Fig. 2. The first important observation is that IEZs can form in the presence of AGD. Secondly, the flow fields within and outside the IEZ are a result of the competitive interaction between current-bedform driven flow and ambient groundwater discharge. The results for both gaining and losing conditions are elaborated below.

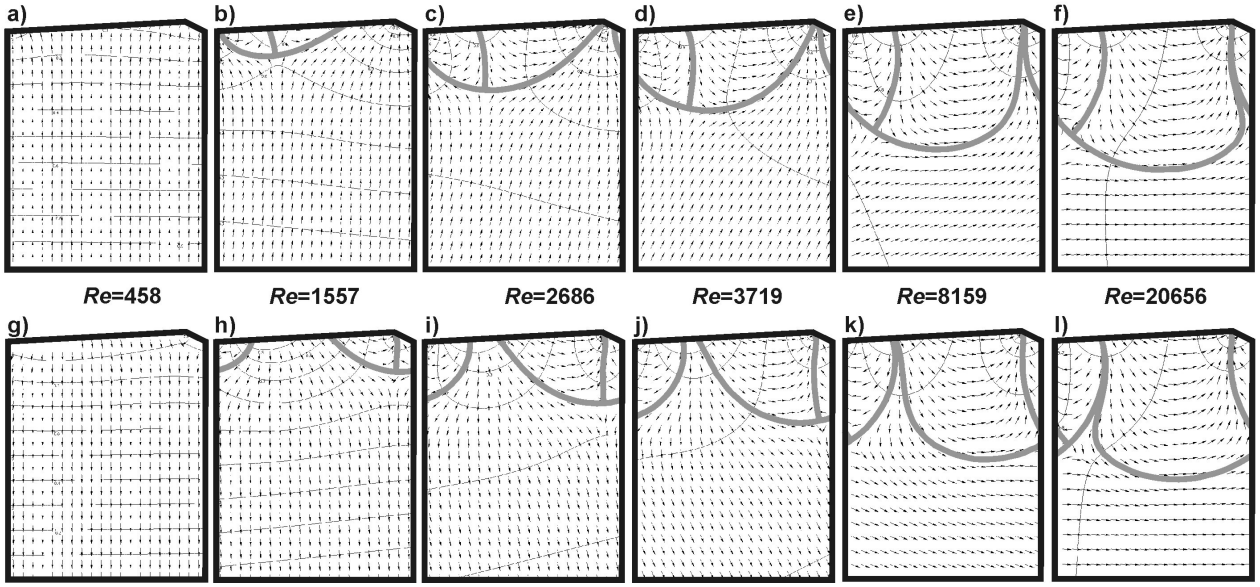

Fig. 2 Top row: pressure fields (contours with intervals of 0.1) and flow directions (arrows) in the sediments for gaining conditions ($q_{bas}^* = 9.8 \times 10^{-2}$) at different Reynolds number (Re). Bottom row: the same for losing conditions ($q_{bas}^* = -9.8 \times 10^{-2}$). Pressure is normalized as: $p^* = (p - p_{min})/(p_{max} - p_{min})$ where p^* is normalized pressure, p is pressure and p_{max} and p_{min} the maximum and minimum pressures for each simulation, respectively. The grey streamlines delineate the interfacial exchange zones. H/L = 0.05 and L = 1.0 m for all cases where H is the bedform height and L is its length.

IEZ spatial configuration and fluxes: gaining conditions

For "gaining" conditions with upward AGD, the IEZ, when it is present, is centred around the bottom-pressure maximum which is located along the stoss or upstream-facing surface of the dune (Fig. 2, top row). This maximum pressure point is located

approximately where the water-column eddy re-attaches (see figures and discussion in Cardenas & Wilson, 2007a). There are two flow cells in the sediments, similar to cases without AGD (Cardenas & Wilson, 2007a). For lower *Re*, the IEZ terminates at points along the SWI that are between the location of the bottom-pressure maximum and the pressure minimum located at the crest (e.g. Fig. 2(b)). These termination points move closer to the crest as the *Re* increases, with the AGD becoming more focused towards the crest. For high *Re* these points almost coalesce, but a thin streamtube still connects the AGD to the pressure minimum near the crest; eventually the IEZ becomes similar to that without AGD (compare to Fig. 7 in Cardenas & Wilson (2007a)). Figure 2(a)-(b) also suggests the presence of a threshold or critical Reynolds number, Re_{crit}, below which there is no IEZ and the sediments are completely filled with discharging deep groundwater. Below Re_{crit}, the dominant vertical pressure gradients result in essentially one-dimensional flow upwards (Fig. 2(a)). Just above Re_{crit}, the IEZ is very sensitive to *Re* (Fig. 2(b)). For much larger Reynolds numbers, current-bedform driven flow dominates and the IEZ approaches its asymptotic depth (Fig. 2(f)), similar to the base case without AGD.

Following Cardenas & Wilson (2007a), a curve-fitting algorithm was used to find a functional expression for the simulated interfacial depth, $d_z(Re)$. Simulations and fits are plotted on the left side of Fig. 3. The Morgan-Mercer-Flodin (MMF) growth model (Morgan *et al*., 1975), $d_z/L = (ab + cRe^d)/(b + Re^d)$, consistently provides good fits ($R^2 > 0.99$) to the simulation results for all values of q_{bas}. The *x*-intercept of the fitted MMF models, *a*, represents Re_{crit}. As shown in these plots and in Fig. 2, the IEZ depth, d_z, approaches an asymptotic, maximum depth at high *Re*. That maximum depth is always less than ~0.75*L* and is less for higher AGD. The flux density through the IEZ, q_{int}*, is plotted on the right side of Fig. 3. It continually increases with *Re*, following a power model, for all values of AGD. This resembles the model fit for the no-AGD relationship (Cardenas & Wilson, 2007a).

IEZ spatial configuration and fluxes: losing conditions

When AGD is downwards along the bottom boundary, the water column is losing water to deep groundwater. Looking only at IEZ depth, d_z, as a measure of the IEZ, there is almost no discernable difference between losing (Fig. 3, bottom row) and gaining (Fig. 3, top row) conditions across varying q_{bas}*. The simulations can again be fitted with an MMF model ($R^2 > 0.99$) with an asymptote. The dependence of IEZ flux density q_{int}* on *Re* for various q_{bas}* conditions is likewise similar between gaining and losing conditions (compare top and bottom of right column in Fig. 3).

Differences, however, are apparent when viewing the flow-field configuration, as shown in Fig. 2. Under losing conditions, the IEZ is centred around the bottom-pressure minimum at the crest (Fig. 2, bottom row), whereas it is centred around the pressure maximum for gaining conditions (Fig. 2, top row). The termination points of the IEZ along the SWI are areas where water is flowing down into the IEZ for the losing scenario; these are areas where water is flowing up into the water column for the gaining case. These termination points get closer to each other with increasing *Re* until, for the losing case, they almost coalesce at the location of the bottom-pressure maximum and the IEZ again looks similar to the non-AGD case. AGD from the

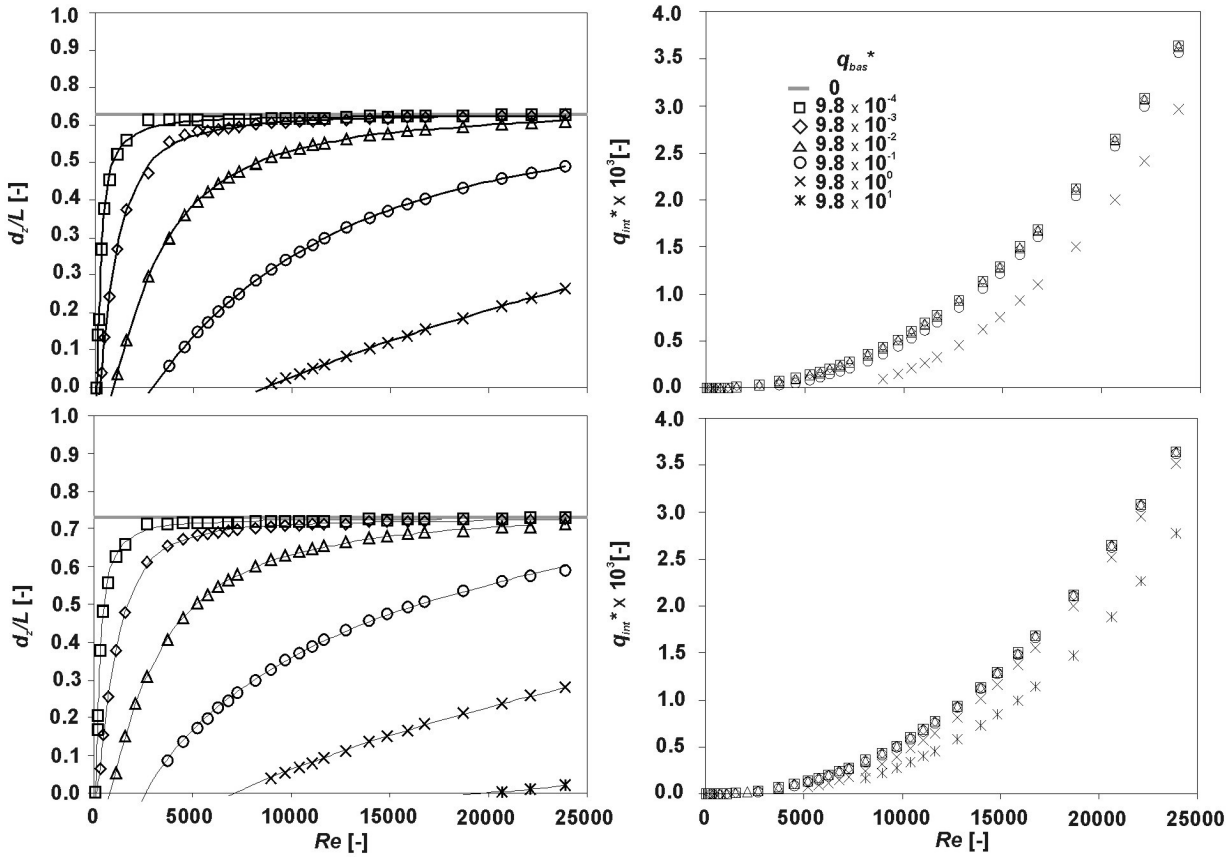

Fig. 3 Dimensionless interfacial exchange zone (IEZ) normalized depths and interfacial fluxes plotted as a function of Reynolds number (*Re*) for different q_{bas}* for gaining (top) and losing (bottom) cases. The horizontal grey lines in the left-hand graphs indicate the IEZ depth for the base case without ambient groundwater discharge (Cardenas & Wilson, 2007a). The solid curves are Morgan-Mercer-Flodin fits to the simulation results. The plots with the open triangles correspond to the simulations shown in Fig. 2. H/L = 0.05 and L = 1.0 m for all cases.

overlying water column is focused into a narrow streamtube that originates around the pressure maximum at the SWI (Fig. 2(l)).

There is also a threshold Re_{crit} for losing conditions. When the downward AGD is dominant, there is no return flow to the SWI (Fig. 2(g)) and all water downwelling from the water column flows towards deeper groundwater. As *Re* increases, the lateral pressure gradient along the SWI becomes sufficiently large such that some of the downwelling water near the bottom-pressure maximum is influenced by the pressure minimum and flows up towards it, returning to the SWI and creating a local IEZ, instead of following the ambient downward flow.

Exchange zone residence times for both cases

Mean residence times, t_r, of fluids flowing through the IEZ can be readily computed from the IEZ flux and porous area, $t_r = nA_z / q_{\text{int}} L$, where is the mean residence time, n is porosity, and IEZ area, A_z, is defined by the SWI and the bounding streamlines that

surround all water originating from and returning to the SWI (Fig. 1). We studied dimensionless mean residence time, defined by $t_r^* = t_r K/nL$, as a function of *Re* and q_{bas}^*, for both gaining and losing conditions (not shown). We found that residence time is large at low *Re*s and decreases rapidly with *Re*. Even though the IEZs are smaller in extent at low *Re*, the fluxes are so small that it takes a long time for fluids to circulate through these small zones. AGD decreases the IEZ residence time, with a larger decrease for lower *Re*. At the lowest *Re* the decrease is exceptionally large. Residence time eventually approaches 0 as the *Re* approaches its critical value, when there is no current-bedform driven exchange and the IEZ shrinks to zero (Fig. 2(a),(g)). We also studied residence time distribution and found it to be fractal (not shown).

SUMMARY

Currents interact with bedform topography to drive advective-interfacial exchange across the sediment–water interface (SWI). The interfacial exchange zone (IEZ) is the area within the sediments characterized by local (0.1–10 m) downwelling and upwelling of seawater, with streamlines originating and ending at the SWI. Current-bedform driven advection of water through the sediments is further complicated by the presence of ambient groundwater discharge (AGD), the upwelling of deeper groundwater, such as in coastal areas influenced by regional (0.1–10 km) submarine groundwater discharge, or the deeper, regional downwelling of seawater intruding into aquifers. Hydrogeologists refer to these two situations relative to whether the water column is "gaining" or "losing" regional flow, respectively. This paper describes the hydrodynamics of IEZs under the joint influence of current-bedform driven exchange and AGD using high-fidelity multiphysics numerical models. We simulate turbulent flow above the SWI and Darcy-groundwater flow below the SWI.

The simulations show that IEZ can develop even in the presence of AGD, under both gaining and losing conditions, provided that the forcing due to current-bedform interaction is sufficiently strong. The competition between current-bedform interaction forcing and AGD forcing controls the IEZ shape, depth, fluxes, and residence times. The IEZ spatial extent (depth and area) increases with current Reynolds number (*Re*) but is diminished by ambient groundwater discharge (AGD) for both gaining and losing conditions. As current *Re* increases, the IEZ depth, area and shape are asymptotic to those for neutral conditions (where the water column is not gaining or losing). The relationship of IEZ depth and area to *Re* is described by simple (MMF) functional models no matter what the relative magnitude of AGD. Under gaining conditions, the IEZ is centred around the bottom-pressure maximum, which is located on the stoss face of dunes, near where the eddy in the water column re-attaches. The deep groundwater upwells near the bottom-pressure minimum which is located at the crest. Under losing conditions, the IEZ forms around the pressure minimum at the crest. Seawater entering the sediments near the bottom-pressure maximum, along the stoss face, downwells into the deep groundwater below the sediments and does not return to the SWI.

The IEZ flux and the mean residence time both depend on current *Re*. Flux increases with *Re* (following a power law), while residence time decreases. Ambient

groundwater discharge (AGD) reduces IEZ flux and residence time, for both gaining and losing conditions.

Our high-fidelity multiphysics numerical modelling study shows that current-bedform driven exchange interacts and competes with ambient groundwater discharge to control the hydrodynamics below sediment–water interfaces. Understanding the hydrodynamics opens a door towards an integrated physical–biological–chemical perspective of biogeochemical and ecological processes along sediment–water interfaces, as well as interfaces with other porous bottom materials including coral and debris.

We have submitted for publication elsewhere a much more detailed account of interfacial exchange when AGD competes with the effects of turbulent current-bedform driven exchange (Cardenas & Wilson, 2007c), including the influence of varying bedform shape.

Acknowledgements This research was funded by an AGU Horton Research Grant and a New Mexico (NM) Water Resources Research Institute Student Grant. MBC was supported by the Frank E. Kottlowski Fellowship of the NM Bureau of Geology and Mineral Resources at the NM Institute of Mining and Technology. We acknowledge technical support by Comsol, Inc. and ESI-Group.

REFERENCES

Boudreau, B. P., Huettel, M., Forster, S., Jahnke, R. A., McLachlan, A., Middelburg, J. J., Nielsen, P., Sansone, F., Taghon, G., Van Raaphorst, W., Webster, I., Weslawski, J. M., Wiberg, P. & Sundby, B. (2001) Permeable marine sediments: overturning an old paradigm. *EOS* **82**, 133–136.

Burnett, W. C., Bokuniewicz, H., Huettel, M., Moore, W. S. & Taniguchi, M. (2003) Groundwater and pore water inputs to the coastal zone. *Biogeochemistry* **66**, 3–33.

Cardenas, M. B. & Wilson, J. L. (2006) The influence of ambient groundwater discharge on exchange zones induced by current-bedform interactions. *J. Hydrol*. **331**, 103–109. doi:10.1016/j.jhydrol.2006.05.012.

Cardenas, M. B. & Wilson, J. L. (2007a) Dunes, turbulent eddies, and interfacial exchange with permeable sediments. *Water Resour. Res*. (in press).

Cardenas, M. B. & Wilson, J. L. (2007b) Hydrodynamics of coupled flow above and below a sediment–water interface with triangular bed forms. *Adv. Water Resour.* **30**, 301–313, doi:10.1016/j.advwatres.2006.06.009.

Cardenas, M. B. & Wilson J. L. (2007c) Exchange across a sediment-water interface with ambient groundwater discharge. *J. Hydrol*. (in press).

Huettel, M., Roy, H., Precht, E. & Ehrenhauss, S. (2003) Hydrodynamical impact of biogeochemical processes in aquatic sediments. *Hydrobiologia* **494**, 231–236.

Morgan, P. H., Mercer, L. P. & Flodin, L. W. (1975) General model for nutritional responses of higher order mechanisms. *Proc. Nat. Acad. Sci. USA* **72**, 4327–4331.

Riedl, R. J., Huang, N. & Machan, R. (1972) The subtidal pump: a mechanism of interstitial water exchange by wave action. *Mar. Biol.* **13**, 210–221.

Webster, I. T., Norquay, S. J., Ross, F. C. & Wooding, R. A. (1996) Solute exchange by convection within estuarine sediments. *Est. Coast. Shelf Sci.* **42**, 171–183.

Wilcox, D. C. (1991) A half century historical review of the k-ω model. *AIAA Paper 91-0615*, Reston, Virginia, USA.